

# GEOMATICS FOR SLOPE STABILITY AND ROCK FALL RUNOUT ANALYSIS: A CASE STUDY ALONG THE ALTA TAMBURA ROAD IN THE APUAN ALPS (TUSCANY, ITALY)

RICCARDO SALVINI & MIRKO FRANCONI

University of Siena - Department of Environment, Earth and Physical Sciences and Centre of Geotechnologies - Siena, Italy

## ABSTRACT

With increasing awareness of geological risks, the study of rocky slopes plays a key role in the Earth Sciences, especially in areas of high vulnerability due to the presence of human settlement. The present paper describes the stability and runout analyses carried out along the Alta Tambura road, in correspondence with the Guadine village connecting the Massa urban settlement to the Apuan Alps (Tuscany, Italy). The integration among various types of survey and analytical methodologies allowed for the application of up-to-date approaches for hazard assessment. Results from these types of studies are useful in the decision-making process concerning choosing the most appropriate mitigation works and, as in such a case, their a posteriori validation. With regard to the survey techniques, terrestrial laser scanning and digital close-range photogrammetry were used to produce the digital elevation model, oriented stereo-images, orthophotos and accurate positions and volumes of rocky wedges and joints located on the slope overhanging the analyzed road. Thanks to this data, a deterministic stability analysis was conducted and the spatial distribution of rock fall density, velocities and kinetic energies was modeled by means of the “cone-method”. Historical evidence of rock falls, identified during fieldwork activities and photointerpretation, were used to assess and calibrate the accuracy of results obtained from the method and allowed, through a further 2D rock fall runout analysis, the calculation of the dissipation energy that protection measures need to mitigate the risk in the area.

**KEY WORDS:** rock topple, runout, photogrammetry, laser scanning, GIS

## INTRODUCTION

The present research started in 2007 when, after a rock fall event occurred during the night of February 27-28 in the Guadine village area (Fig. 1), the Massa Municipality decided to conduct a detailed study on the stability of the slope overhanging the Alta Tambura road. The road connects Massa to five villages of the Apuan Alps - Guadine, Gronda, Redicesi, Casania and Resceto, which were isolated for several days because of the main street destruction due to the event. The presence of large angular boulders at the bottom of the valley implies that this area has already experienced

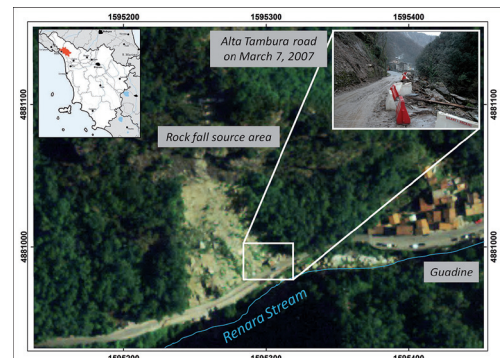


Fig. 1 - Orthophoto of the Guadine village showing the zone affected by rock fall in 2007, and highlighting Alta Tambura road on March 7, 2007; inset map of Tuscany showing the Apuan Alps in red

rock falls, leading to serious problems for the road.

The aim of this study is to acquire detailed geological and topographical information which, together with climate and chemical weathering, induce rock fracturing, opening of joints, rainfall infiltration, and subsequent instability (LIM *et alii*, 2004). Once the failure process initiates, the rock detaches and the falling trajectory is dictated by slope geometry and land use. The lack of detailed data on slope topography, instability source areas, rock block geometry and falling paths, including runout distance, can limit the assessment of rock fall hazard (DORREN, 2003, GLENN *et alii*, 2006). In order to obtain all the information necessary to perform the slope stability analysis and the rock fall runout simulation, several types of geomatic surveys and analytical methodologies were proposed. In this paper, we used Digital Terrestrial Photogrammetry (DTP) and Terrestrial Laser Scanning (TLS) to study the geometric characteristics of slopes, rocky wedges and discontinuities, thus overcoming problems like the inaccessibility of outcrops and the complexity of the slope morphology. Today, TLS is one of the best ways to characterize the rock mass (FEKETE *et alii*, 2010; TAMBURI, 2008; NGUYEN *et alii*, 2011; RUNQIU & XIUJUN, 2008), to analyze the slope stability (ARMESTO *et alii*, 2009; NAGALLI *et alii*, 2012; KASPERSKI *et alii*, 2010), and to model the rock fall (ABELLÁN *et alii*, 2010; OPIKOFE *et alii*, 2009; MONNET *et alii*, 2010). DTP also provides information about the structural and geo-engineering setting of slopes. Since the 1970s, photogrammetry has been utilized to characterize the rocky mass (WICKENS & BARTON, 1971; MOSAAD ALLAM, 1978) and nowadays, thanks to the advance of digital and informatic methodologies, it has become widespread either with (FERRERO *et alii*, 2009; STURZENEGGER & STEAD, 2009; SALVINI *et alii*, 2011; SALVINI *et alii*, 2013) or without TLS (HANEBERG, 2008; RONCELLA *et alii*, 2005; STURZENEGGER *et alii*, 2009; FIRPO *et alii*, 2011).

The geomatics technologies used can yield oriented stereo-images, orthophotos and precise digital models of slopes and rocky wedges. Geometrical and structural characteristics of slopes, such as joint attitude, spacing and persistence, and block volumes, can be also derived. The results were used together with a deterministic method to evaluate the slope stability. Through the application of the “cone-method” (TOPPE, 1987; JABOYEDOFF & LABIOUSE, 2003; JABOYEDOFF *et*

*alii*, 2005) we assessed the probabilistic distribution of rock fall end points, velocity and kinetic energy along the rock falling paths and existing barriers. By modeling the spatial distribution of rock fall frequency, we improved the accuracy of the study moving from a 2D analysis, which assumes that the fall follows the path of steepest descent, to a 2.5D approach.

## GEOLOGICAL AND GEOMORPHOLOGICAL SETTING

In the rock fall area and at the base of the Renara stream, outcrops are composed of lithotypes belonging to the Paleozoic Crystalline Basement of the Apuan “Autochthonous” (CARMIGNANI, 1985) which consists of the “Porphyroids and porphyric schists” and the “Lower Phyllites” formations. Porphyroids are made of rhyolitic-rhyodacitic metavulcanites, are either light green or gray in colour, with millimeter crystals of quartz and feldspars in a quartzitic, muscovitic and chloritic matrix. Porphyric schists are characterized by muscovitic-chloritic fillads and metarkoses with abundant quartzitic porphyroclasts. The “Grezzoni” formation crops out on the slope, above the crystalline basement. Thin and discontinuous lenses of “Seravezza Breccias” and “Megalodon marble” separate this formation from the overlying “Dolomitic marble”, which is made of light gray-pinky dolomite alternating with dolomitic marble. Such a geological sequence belongs to the “Autochthonous” Unit and crops out in the overturned limb of the “Vinca-Forno” anticline, a non-cylindrical isoclinal NE-vergent fold, formed during the first compressive deformation event (D1 phase) and dated as late Oligocene - very early Miocene (CARMIGNANI & KLIGFIELD, 1990). Since the early Miocene, a second deformation phase (D2) overprinted the earlier structures, generating new ductile to ductile-brittle (and later only brittle) structures linked to post-compression tectonic uplift and internal extension of the piled-up tectonic units. In the study area, the folds generated during the D2 phase show axes oriented at N300° and dips gently towards the NE

With regard to the geomorphology, the study area is strongly influenced by the structural-geological arrangement of the Apuan Alps. The area belongs to the M. Cipolla - M. Girello ridge characterized by a SW-NE direction and by a very sharp crest, which varies in elevation between 630 and 930 m a.s.l.. The upper part of the ridge is composed of carbonaceous rocks

with a high slope gradient, and the intermediate and lower parts of the slope consist of rocks belonging to the crystalline basement with a lower slope gradient. In addition to the slope gradient, type and presence of the vegetation also influences the structural-geological arrangement of the area; in fact, it was observed that slopes appear rockier with the discontinuous vegetation in the highest part of the ridge, while dense forest and soil cover is more prevalent in the lower part of the slope. This type of morphology is quite common in the Apuan Alps, as documented by literature with studies on the influence of the geological-geomorphological setting on landslides (BARONI *et alii*, 2010; D'AMATO AVANZI *et alii*, 2000).

The rock fall occurred on the lower part of the ridge, with the slope having a mean dip of approximately  $38^\circ$  and a rectilinear-convex profile, which, according to LEHMAN (1756), can be classified as a "rectified slope". The outcropping rocks in this area experience strong physical weathering dominantly caused by intense rainfall events. In fact, the meteoric affluxes are very heavy in the Apuan Alps, with a mean annual rainfall of over 3,000 mm (D'AMATO AVANZI *et alii*, 2004). This pluvio-metric regime is controlled by the particular climate of the Apuan Alps, referred to as the Apennine-Mediterranean type, with transition to the sub-coastal type, characterized by dry summers and cold winters, with a primary peak of rainfall in the autumn and two secondary maximums in the winter and spring. This extreme climate feature is related to the location and the shape of the Apuan Alps, which intercept air flow originating from the Atlantic to the west or the Mediterranean, and produce the forced lifting of humid air masses, favoring their rapid adiabatic cooling (D'AMATO AVANZI *et alii*, 2004). The physical weathering acting in the area, together with karst phenomena associated with the geology, are conducive to slope instability, thus generating rock falls and debris deposits accumulation in the morphological depressions. Along the SE slope of the ridge, several nivation niches host debris deposits that occasionally fail, while the NW slope shows nivation hollows referable to the last Pleistocene glaciation (BINI, 2005; FEDERICI, 2005).

The Guadine event was interpreted as an effect of physical weathering of porphyroids and porphyric schists through surface processes, generating rock falls on the steepest slopes. The rock debris deposits are at the limit of equilibrium and can be mobilized after concen-

trated rainfall events, alternated by dry periods. Studies carried out for the rock fall immediately following the event occurred on February 27-28 (SALVINI *et alii*, 2007a; SALVINI *et alii*, 2007b) and additional in-depth analyses performed by the Massa Municipality resulted in the installation of several protectionary measures (Fig. 2) such as beams, bars and inelastic and elastic barriers both in the upper and lower part of the slope. Elastic barriers, installed in 2010, are certified (E2000), 4 meters high and able to support up to 2,000 kJ

## MATERIALS AND METHODS

With the aim of understanding the geological setting of the slope and the consequent rock fall causes, a new geological map with instability landforms at a scale of 1:5,000 was produced (Fig. 3) based on field-work surveys, existing literature (CARMIGNANI, 1985; CARMIGNANI & KLIFFIELD, 1990; DI PISA *et alii*, 1985) and the official map of the Tuscany Region at a scale of 1:10,000 (249110 section).

Moreover, engineering-geological surveys were carried out in such a way as to have a complete understanding of the joint systems necessary to perform the stability analysis of latent blocks. In addition to traditional geological, geomorphological and engineering-geological surveys, DTP and TLS were used to carry out a detailed analysis of discontinuities and wedges throughout the slope, particularly in inaccessible areas. The photogrammetric survey was executed using a reamed bar mounted on a topographic tripod set on the slope facing the one under study. The distance between the zone of data acquisition and the slope was ca. 300 m, thus requiring two digital cameras, Canon™



Fig. 2 - Examples of protectionary measures executed by the Massa Municipality



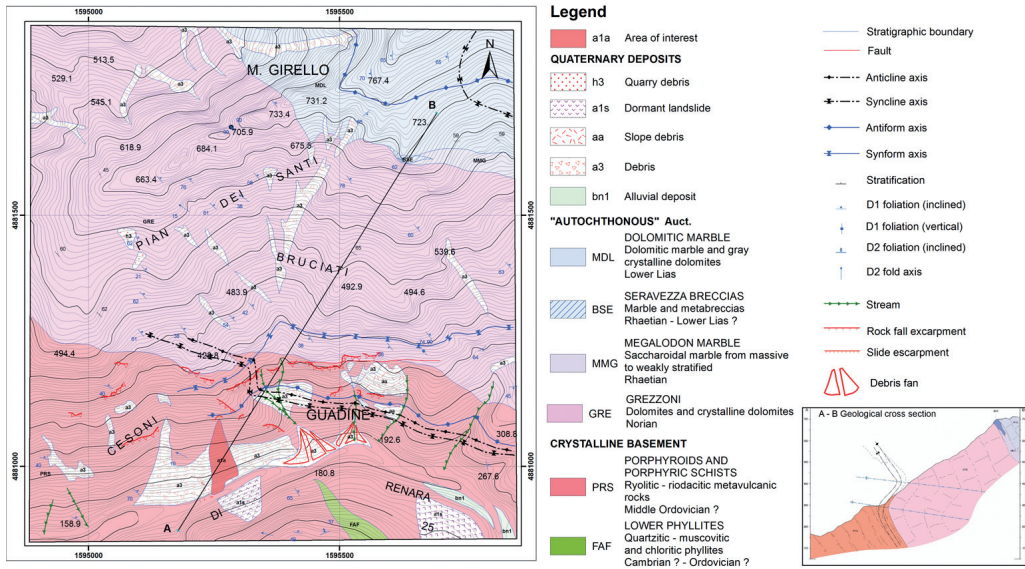


Fig. 3 - Geological map showing instability landforms and a cross section; (black-colored fold axes represent minor structures of D1 phase within the "Vinca-Forno" anticline; blue-colored structures relate to antiform and synform axes of the D2 phase refolding of the primary schistosity)

Eos5D and Eos20D, with focal lengths varying from 10 to 200 mm to produce detailed and panoramic photos. The resolution of the two cameras was set to 14 and 8 Megapixel, respectively. The direction of strips was oriented parallel to the slope as much as possible, at N65, with pitching at approximately  $\pm 15^\circ$  from the horizontal in order to have a complete photographic coverage of the unstable slope.

Differential GPS and topographic surveys were also carried out in order to collect Ground Control Points (GCP), that were clearly visible on the slope and necessary for the absolute orientation of the images. A Leica™ TCRP 1203+R1000 (reflectorless) total sta-



Fig. 4 - Topographic surveying with the total station (A); TLS during data acquisition (B)

tion and two Leica™ System 1200 GPS receivers were used for the topographic survey (Fig. 4A). Through the GSM connection to the Leica Geosystems™ SpiderNet network, differential GPS techniques were applied with the aim of determining the absolute coordinates of the system origin, and that of the azimuth zero direction. By this technique, since the total station allowed for determination of the relative coordinates of surveyed points (X, Y and Z) through the measurement of angles and distances and trigonometric calculations, absolute coordinates of ca. 100 GCP were calculated and used for the absolute orientation of the images within LPS module of ERDAS™ IMAGINE software.

Moreover, a Riegel™ Z420i TLS (Fig. 4B) was used to acquire a point cloud necessary for the 3D modelling of the slope. The distance between the slope and the instrument ranged from 250 to 400 m and the spatial resolution of the point cloud was set to 7 cm at a distance of 300 m, corresponding to a scanning angle of  $0.013^\circ$ . The point cloud was stored and processed using Leica™ Cyclone software. The described topographic survey was also utilized for the registration to absolute coordinates of the TLS point cloud.

Data was analyzed by DTP and 3D modelling techniques that, managed within a Geographical Information System (GIS), constructed a complete deterministic understanding of the geometric charac-

teristics of slopes, wedges and joints. These, together with engineering-geological fieldwork measurements, allowed for the analysis of the stability of the slope and the rock fall runout.

Kinematic analyses of stability were carried out using joint systems so that latent phenomena could be geometrically identified. Dips. 6.0 software (Rocscience™) was used for this deterministic study, using friction angles from the engineering-geological survey and several slope attitudes as computed from spatial processing of the Digital Elevation Model (DEM). The DEM was created from TLS data which was merged to morphological features, which were stereo-restituted from terrestrial and aerial photographs, and altogether were merged to the existing topographic maps at a scale of 1:2,000; this activity was necessary to fill shadows that resulted in the point cloud in proximity to vegetated areas and at the toe of the slope near the stream bed. The final DEM was created in grid format with a 1 m cell size. Spatial analysis techniques were applied to the DEM in order to obtain the slope and the aspect of different slope zones, giving the dip and dip direction to be utilized in the stability analysis. Spatial variability of the slope morphology was then used for the purpose of studying the steadiness of several dipping slopes, up to the computed maximum stable slope angles.

Results from the kinematic stability analysis highlighted a critical joint system conducive to toppling. Hence, we performed a dynamic study using the beta testing version of the RocTopple software (Rocscience™), which is based on the GOODMAN & BRAY method (1976). The study was carried out under both static and dynamic conditions, dependant on the local seismic acceleration and the percentage of water saturation. We derived seismic coefficients (dimensionless numbers that define the seismic acceleration as a fraction of the acceleration due to gravity) from the GeoStru PS software (GEOSTRU, 2008), obtaining values of 0.099 and

0.049 for the horizontal and vertical acceleration, respectively. The percentage of water saturation in joints was empirically varied from 0 to 100%. The procedure was carried out in accordance to the Italian Norme Tecniche per le Costruzioni (NTC) (M.LL.PP., 2008). In addition to the deterministic study, a probabilistic and sensitivity analysis on Safety Factor (SF) related to the critical joint system was performed with the aim of defining its variation as combination of input variables, as shown in Tab. 1.

Taking into account the presence of the road and the houses at the bottom of the slope, results of the stability study were integrated with a detailed rock fall runout analysis based on the DEM. The analysis was conducted by means of RocFall software (Rocscience™).

The “cone-method” was applied through the free-ware Conefall software (Quanterra™) in order to calculate the spatial distribution of rock fall transit density, velocities and kinetic energy. This required the usage of the DEM and the source position of the most dangerous blocks sited on the slope, which were identified through the photointerpretation of terrestrial photos. Results were used to validate the dispersion areas and to create proper rock fall trajectories. This method maps the general rock fall spatial distribution and is helpful in understanding which areas could be affected by a hypothetical rock fall. However, values obtained from these simulated rock fall events were calculated based on all the blocks sited on the slope in this study, so the real velocity and kinetic energy which could be reached during a fall could not be determined for each individual block. Hence, with the aim of trying to overcome such a limitation, the method was calibrated by calculating the volume of rocky blocks present at the bottom of the valley, which are remnants of past failures from the slope. This was conducted using fieldwork data and evidence from photointerpretation. This, in combination with a further 2D rock fall simulation, allowed us to better assess the kinetic energy of blocks during the fall and, consequently, the dissipation energy that protection measures should have in order to effectively mitigate the risk of similar collapses.

## RESULTS

The cognitive survey shows that the 2007 rock fall originated from an elevation of 316 m a.s.l., forming a detachment niche 18 m wide. The rock fall reached the Renara stream bed at an elevation of 180

| VARIABLE                           | INPUT VALUE | LOWER LIMIT | UPPER LIMIT |
|------------------------------------|-------------|-------------|-------------|
| Slope Height (m)                   | 150         | 120         | 165         |
| Slope Angle (°)                    | 43          | 34          | 45          |
| Upper Slope Angle (°)              | 0           | 0           | 50          |
| Bedding Width (m)                  | 2           | 1.5         | 3           |
| Bedding Dip (°)                    | 77          | 75          | 85          |
| Joint Friction Angle (°)           | 30          | 25          | 35          |
| Joint Cohesion (t/m <sup>2</sup> ) | 0.04        | 0           | 0.2         |
| Joint Percent Fill Pore Pressure%  | 50          | 0           | 100         |

Tab. 1 - Variables and relative ranges used in the probabilistic study on SF

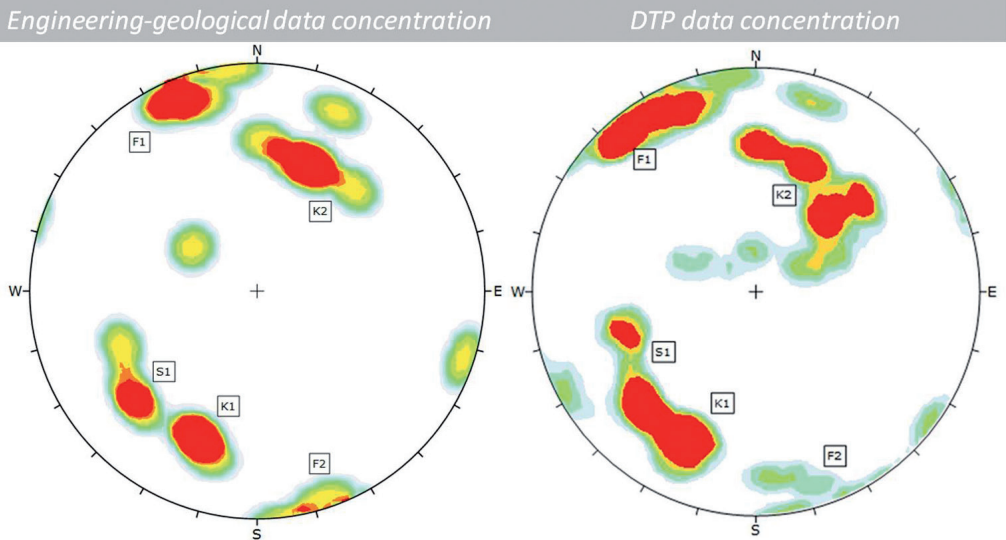


Fig. 5 - Contour plots of joint systems from engineering-geological survey and DTP. Data is presented using stereographic projection through the Schmidt equal-area method

m a.s.l., overtopping a 90 m long stretch of the Alta Tambura road.

The study revealed that the landslide originated as a rock topple involving boulders and soil in proximity to an hold trail which was characterized, in that part, by a dry stone wall. Rainfall events in the days preceding the landslide led to initial failure triggered by poor drainage and an increase of water pressure at the interface between debris and rocky basement. Toppling of rock down the steep slope by bouncing, rolling and sliding then increased the volume of the failed mass, clearing the slope of soil, debris and stones in unstable equilibrium and destroying the old anthropic terraces which characterized the slope from 250 to 185 m a.s.l.. The mechanism which caused such an event represents one of the most

critical geomorphologic vulnerabilities of the zone, prone to rock toppling and to the difficulties of controlling the water runoff.

The integration of geomatics and traditional engineering-geological surveys allowed for the determination of the attitude of joint systems and slopes. Measurements from DTP were compared with fieldwork data by means of a density analysis of attitudes in stereographic projection (Fig. 5). As shown in the figure, similarities between the joint distribution obtained through engineering-geological surveys and DTP are evident, even if the photogrammetric data have a greater dispersion. This is because the engineering-geological survey was carried out in accessible outcrops, whereas DTP photointerpreted joints refer to the whole 3 ha wide slope. The larger the area under study, the more the attitude of joints may vary. Nevertheless, the mean attitude derived from the two methods corresponds well with data variability that is always less than  $10^\circ$  (Tab. 2).

| JOINT SYSTEM | MEAN ATTITUDE             |               |
|--------------|---------------------------|---------------|
|              | Geo-engineering (degrees) | DTP (degrees) |
| F1           | 160/79                    | 155/78        |
| F2           | 345/83                    | 342/79        |
| S1           | 53/58                     | 59/52         |
| K1           | 21/58                     | 25/60         |
| K2           | 202/52                    | 206/50        |

Tab. 2 - Mean values of joint systems attitude from geo-engineering survey and DTP

| Slope (Dip Direction/Dip) | F2 apparent dip | SF   | SF (50% saturation) | SF (sc) | SF (sc + 50% saturation) |
|---------------------------|-----------------|------|---------------------|---------|--------------------------|
| 125/43                    | 77              | 0.98 | 0.9                 | 0.89    | 0.83                     |
| 140/40                    | 79              | 2.99 | 1.95                | 1.97    | 1.42                     |
| 160/40                    | 80              | 3.30 | 2.08                | 2.11    | 1.50                     |
| 180/40                    | 79              | 2.99 | 1.95                | 1.97    | 1.42                     |
| 205/43                    | 77              | 1.01 | 0.93                | 0.92    | 0.84                     |

Tab. 3 - Variation of SF in different slopes taking into account water saturation in joints and local seismic acceleration (sc=seismic coefficients)



Based on slope morphology as measured from the DEM, the kinematic stability analysis was conducted by testing several slopes with dip directions and dips varying respectively from 115 to 160° and from 40 to 60°. The F2 joint system proved positive to toppling failures and the subsequent kinematic analysis, aimed to calculate the slope stability limit angles, gave the following results: if considering 30° of dip direction variability plus a tolerance of 10° because of system scattering, unstable slopes may vary from 125 to 205° in dip direction with a dip of about 13°. When dealing with toppling kinematic analyses, the friction angle (30° for the F2 system) must also be considered to compute the slope limit angle, so that it may finally vary from 125/43 to 205/43.

By means of spatial analysis techniques, these values of dip direction and dip were applied within ArcGIS software (ESRI™) to map the combination between “aspect” and “slope” calculated from the DEM; this processing made it possible to highlight areas potentially prone to this kind of collapse (Fig. 6)

DTP allowed for the identification of the source

points for failures and for the measurement of the volume of the most dangerous blocks located on the slope, yielding sizes ranging from 7 to 500 m<sup>3</sup> and a mean value of 90 m<sup>3</sup>. This was followed by a dynamic stability analysis of the F2 system, which included the computation of the slope stability limit angles. In addition to the geometrical characteristics of slopes and joints, RocToppo also requires input data such as the rock unit weight (2.7 t/m<sup>3</sup>), the shear strength model (Mohr-Coulomb), the joints friction angle (30°) and the cohesion (0.04 t/m<sup>2</sup>). The values used for this computation came from the engineering-geological survey, rock mass classification and literature. Table 3 shows the variation of SF for different slopes up to the slope stability limit angles, taking into account water saturation in joints and local seismic acceleration. It shows that SF is always greater than the physical limit (1.00) with the exception of slope stability limit angles which lie close to or below 1.00, both in static and dynamic conditions. The change of slope dip direction and the relative F2 apparent dip reduction cause the decrease of SF.

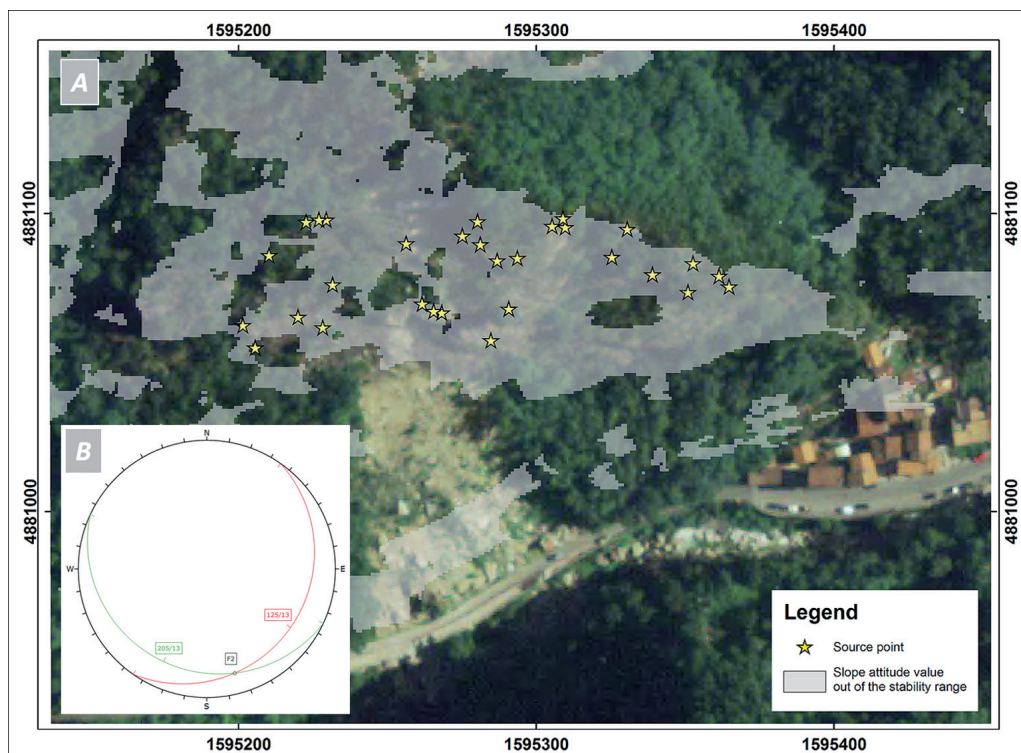


Fig. 6 - Map of source points and areas where the slope attitude values are out of the stability range for F2 joint system toppling (A). Stereographic projection of maximum stable slope angles using the Wulff equal-angle method (B)

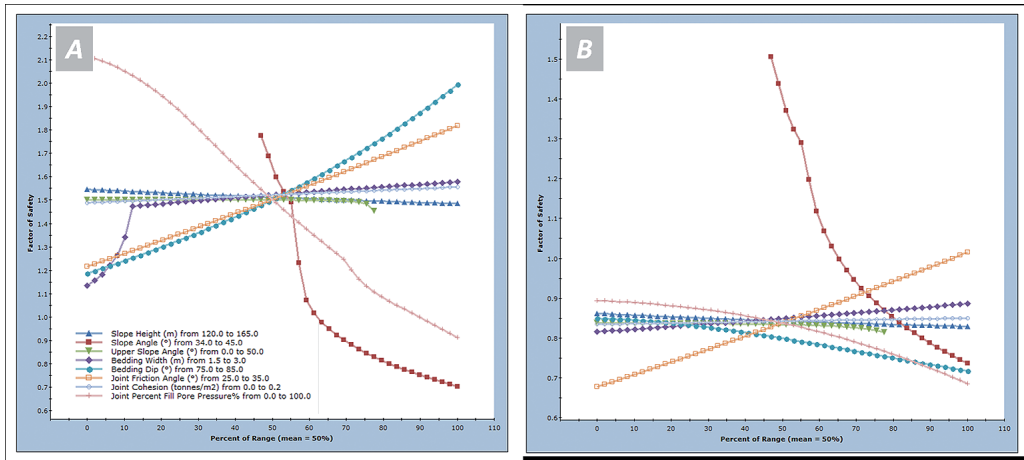


Fig. 7 - Cumulative plots of input variables in the sensitivity analysis of failure; the actual slope 160/40 (A) and the slope stability limit angle 125/43 (B)

The cumulative plots of Fig. 7 show results of the probabilistic sensitivity analysis of failure. The stability of the actual slope (plot A in Fig. 7) is particularly influenced by water saturation in joints and slope angle, confirming the need for proper water management and morphological and land use maintenance. As expected, the stability of the slope limit angles (plot B in Fig. 7 showing the case of the slope oriented at 125/43) is hardly affected by the variability of its dip value and secondly by water saturation in joints and joint friction angle.

The final step of the study was the rock fall runout analysis, which was aimed firstly, at verifying the probability of blocks which were identified of reaching the road and houses and secondly, at establishing the worth of measures of protection necessary to manage the risk. The analysis showed that a wide area located at the bottom of the studied slope could be intensively affected by block fall. Maps of Fig. 8 show: i) the source points of potential rock fall events (Fig. 8A) corresponding to unstable blocks, as defined during the photogrammetric and the stability analyses; ii) the rock fall transit density (Fig. 8B), the rock fall velocity (Fig. 8C) and the rock fall kinetic energy (Fig. 8D).

It is important to emphasize that results do not come only from a 2D runout simulation, which is limited to creating rock fall profiles subjectively and lacks modeling of the lateral trajectory dispersion, but from a combination with the “cone-method” which analyses the spatial frequency (JABOYEDOFF *et alii*, 2005). Moreover, as already mentioned, in order to calibrate

the method in terms of rock fall velocity and kinetic energy, all the achieved results were then confirmed through comparison with evidence of rocky blocks collapsed in the past from the slope and recognizable today on the stream bed.

Thus, considering the position and the typology of the barriers installed on and at the foot of the slope, a further 2D runout analysis was carried out with the aim of evaluating the kinetic energy that every single block could potentially have upon impact with the protectionary structures. Fig. 9 shows an example of such an analysis where a block, during ten trials, is successfully stopped by the barriers. Knowing this deterministic energy, it was possible to verify the efficiency of the installed protectionary measures in any different studied zones. Results of this study showed very high values of kinetic energy when simulating the detachment of big blocks located at the top of the slope. The value of impacting energy decreased for smaller blocks or those sited in the lower part of the slope. It is important to underline that the Massa Municipality installed protection barriers which are either double or triple-lined. Therefore, acting together, these barriers could limit even very high rock fall energy (Fig. 9). Considering that the value of kinetic energy was sometimes much larger than one tolerable by the most efficient existing passive protection systems, additional active reinforcements have been adopted and partially completed. This has been possible through the installation of steel cable panels, the attachment of blocks to stable portions of the slope



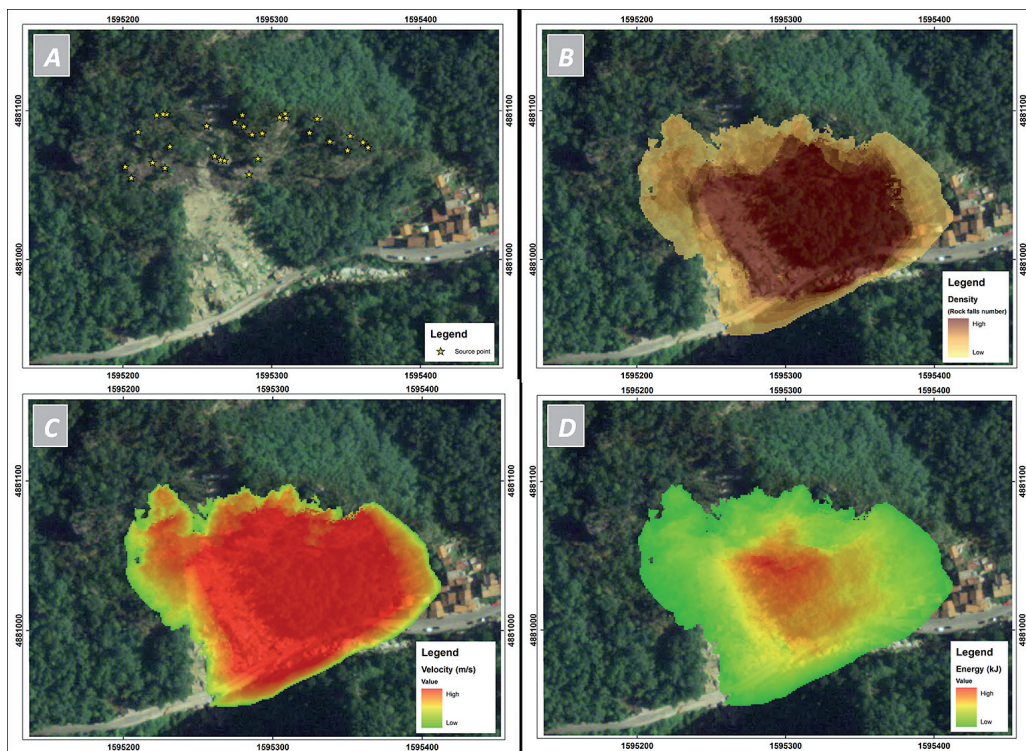


Fig. 8 - Source points of rock fall (A); map of rock fall transit density (B); map of rock fall velocity (C); map of rock fall kinetic energy (D)

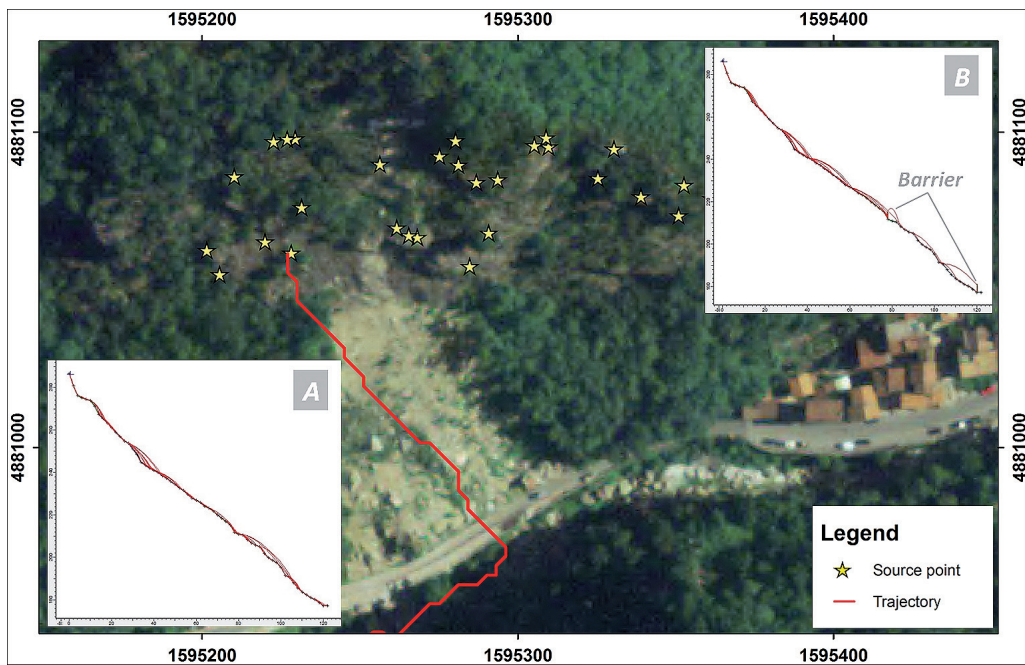


Fig. 9 - Example of a 2D rock fall runout simulation before (A) and after the installation of the protective barriers (B)

through bars, bolts and steel cables and slings, and the creation of more efficient draining systems necessary to avoid water overpressures.

## CONCLUSIONS

Geological and engineering-geological studies, integrated with geomatics surveys, highlight the interconnection between geological setting, geomorphology, meteorological events, climate and slope instability. Under particular climatic conditions and land conservation abandonment, rock blocks and debris deposits could trigger unexpected failures which are then able to evolve into large landslides, as in this case study.

Moreover, this study demonstrated that by interacting with other systems and the slope, the F2 joint system could generate rock blocks prone to toppling, as proven by the presence of large angular boulders at the bottom of the valley.

The attitude of other joint systems, variously dipping towards the slope (i.e. F1, K2), favors water infiltration and, without the creation of more efficient drainage networks, could induce new instability events.

The estimation of the area affected by rock fall was produced through the analysis of the transit density spatial distribution. Based on these results, the subsequent 2D runout analysis enabled calculation of the proper trajectories and determination of the energy that blocks could reach during hypothetical slope rockfall. Knowing the kinetic energy of blocks made it possible to evaluate and assess the efficiency of protection systems which have been installed.

## ACKNOWLEDGMENTS

The authors wish to acknowledge the support by Massa Municipality, geol. Andrea Piccinini and Rocscience Inc.

## REFERENCES

- ABELLAN A., CALVET J., VILAPLANA J.M. & BLANCHARD J. (2010) - *Detection and spatial prediction of rockfalls by means of terrestrial laser scanner monitoring*. *Geomorphology*, **119**: 162-171.
- ARMESTO J., ORDONEZ C., ALEJANO L. & ARIAS P. (2009) - *Terrestrial laser scanning used to determine the geometry of a granite boulder for stability analysis purposes*. *Geomorphology*, **106**: 271-277.
- BARONI C., RIBOLINI A., BRUSCHI G. & MANNUCCI P. (2010) - *Geomorphological map and raised-relief model of the Carrara marble Basins, Tuscany, Italy*. *Geogr. Fis. Dinam. Quat.*, **33**: 233-243.
- BINI M. (2005) - *Glacial landforms in the Apuan Alps (Tuscany -Italy): features in danger of extinction*. *Il Quaternario, Italian Journal of Quaternary Sciences*, **18** (1): 175-178.
- CARMIGNANI L. & KLIGFIELD R. (1990) - *Crustal extension in the Northern Apennines: the transition from compression to extension in the Alpi Apuane core complex*. *Tectonics*, **9**: 1275-1303.
- CARMIGNANI L. (1985) - *Carta geologico-strutturale del complesso metamorfico delle Alpi Apuane (Foglio Nord) - Scala 1:25.000*. LAC - Litografia Artistica Cartografica, Florence, Italy.
- D'AMATO AVANZI G., GIANNECCHINI G. & PUCCINELLI R. (2000) - *Geologic and geomorphic factors of the landslides triggered in the Cardoso T. Basin (Tuscany, Italy) by the June 19, 1996 intense rainstorm*. *Proc. of 8<sup>th</sup> International Symposium on Landslides*: 381-386.
- D'AMATO AVANZI G., GIANNECCHINI G. & PUCCINELLI R. (2004) - *The influence of the geological and geomorphological settings on shallow landslides. An example in a temperate climate environment: the June 19, 1996 event in northwestern Tuscany (Italy)*. *Engineering Geology*, **73**: 215-228.
- DI PISA A., GATTIGLIO M., MECCHERI M. & VIETTI N. (1985) - *Nuovi dati sulle Metabasiti della Valle del Giardino del Basamento Paleozoico Aprano*. *Atti Soc. Tosc. Sc. Nat. Ser.A*, **95**: 89-103.
- DORREN L.K.A. (2003) - *A review of rock fall mechanics and modelling approaches*. *Progress in Physical Geography*, **27**: 69-87.
- FEDERICI P.R. (2005) - *Aspetti e problemi della glaciazione Pleistocenica nelle Alpi Apuane*. *Istituto Italiano di Speleologia. Memorie, Ser.II*, **18**: 19-32.
- FEKETE S., DIEDERICHS M. & LATO M. (2010) - *Geotechnical and operational applications for 3-dimen. laser scanning in drill and blast tunnels*. *Tunnelling and Underground Space Technology*, **25**: 614-628.
- FERRERO A.M., FORLANI G., RONDELLA R. & VOYAT H.I. (2009) - *Advanced geostructural survey methods applied to rock mass characterization*. *Rock Mechanics and Rock Engineering*, **42** (4): 631-665.
- FIRPO G., SALVINI R., FRANCONI M. & RANJITH P.G. (2011) - *Use of digital terrestrial photogrammetry in rocky slope stability*

- analysis by distinct elements numerical methods*. International Journal of Rock Mechanics and Mining, **48** (7): 1045-1054.
- GEOSTRU (2008) - *GeoStru PS Software*. <http://www.geostru.com/geoapp/parametrisismici.aspx> (access date 18 February, 2013).
- GLENN N.F., STREUTKER D.R., CHADWICK D.J., THACKRAY G.D. & DORSCH S.J. (2006) - *Analysis of LiDAR-derived topographic information for characterizing and differentiating landslide morphology and activity*. Geomorphology, **73**: 131-148.
- GOODMAN R.E. & BRAY J.W. (1976) - *Toppling of rock slopes*. ASCE Specialty Conference on Rock Engineering for Foundations and Slopes, **2**: 201-234.
- HANEBERG W.C. (2008) - *Using close range terrestrial digital photogrammetry for 3-D rock slope modelling and discontinuity mapping in the United States*. Bulletin of Engineering Geology and the Environment, **67**: 457-469.
- JABOYEDOFF M., DUDT J.P. & LABIOUSE V. (2005) - *An attempt to refine rock fall hazard zoning based on the kinetic energy, frequency and fragmentation degree*. Nat Hazard Earth Sys, **5**: 621-632.
- JABOYEDOFF M. & LABIOUSE V. (2003) - *Preliminary assessment of rockfall hazard based on GIS data*. 10<sup>th</sup> International Congress on Rock Mechanics ISRM 2003, Technology Roadmap for Rock Mechanics. South African Institute of Mining and Metallurgy, Johannesburg, South Africa, 575-578.
- KASPERSKI J., DELACOURT C., ALLEMAND P., POTHERAT P., JAUD M. & VARREL E. (2010) - *Application of a terrestrial laser scanner (TLS) to the study of the Séchilienne Landslide (Isère, France)*. Remote Sens., **2**: 2785-2802.
- LEHMANN J.G. (1756) - *Versuch einer Geschichte von Flötz-Gebürgeu betreffend deren Entstehung, Lage, darinne befindliche Metallen, Mineralien und Fossilien größtentheils aus eigenen Wahrnehmungen und aus denen Grundsätzen der Natur-Lehre hergeleitet, und mit nöthigen Kupfern versehen*. Berlin, Germany, 76 pp.
- LIM C.H., DEREK MARTIN C. & HERD E.P.K. (2004) - *Rock fall hazard assessment along railways using GIS*. (CD-ROM) Proceedings of the 57<sup>th</sup> Canadian Geotechnical Conference. Quebec City, Canada, 1-8.
- M.L.L.P.P. - MINISTERO DEI LAVORI PUBBLICI (2008) - *NTC Norme Tecniche per le Costruzioni*. D.M. del 14/01/2008. Gazzetta Ufficiale della Repubblica Italiana, 04.02.2008, 15-25 (and pp. 196-198).
- MONNET J.M., CLOUET N., BOURRIER F. & BERGER F. (2010) - *Using geomatics and airborne laser scanning for rock fall risk zoning: a case study in the French Alps*. Canadian Geomatics Conference and Symposium of Commission I (ISPRS). Calgary, Alberta, Canada.
- MOSAAD ALLAM M. (1978) - *The estimation of fractures and slope stability of rock faces using analytical photogrammetry*. Photogrammetria, **34** (3): 89-99.
- NAGALLI A., FIORI A.P., NAGALLI B. & DOS SANTOS IZZO R.L. (2012) - *Terrestrial laser scanning on rock mass stability analysis*. Electronic Journal of Geotechnical Engineering, **17**/Bundle M, 1817-1831.
- NGUYEN H.T., FERNANDEZ-STEGER T.M., WIATR T., RODRIGUES D. & AZZAM R. (2011) - *Use of terrestrial laser scanning for engineering geological applications on volcanic rock slopes - an example from Madeira island (Portugal)*. Nat. Hazards Earth Syst. Sci., **11**: 807-817.
- OPPIKOEFER T., JABOYEDOFF M., BLIKRA L., DERRON M.H. & METZGER R. (2009) - *Characterization and monitoring of the Aknes rockslide using terrestrial laser scanning*. Nat. Hazards Earth Syst. Sci., **9**: 1003-1019.
- RONCELLA R., FORLANI G. & REMONDINO F. (2005) - *Photogrammetry for geological applications: automatic retrieval of discontinuity orientation in rock slopes*. Proceedings of SPIE-IS&T Electronic Imaging, SPIE, **5665**: 17-27.
- RUNQIU H. & XIUJUN D. (2008) - *Application of three-dimensional laser scanning and surveying in geological investigation of high rock slope*. Journal of China University of Geosciences, **19**: 184-190.
- SALVINI R., FRANCONI M., FANTOZZI P.L., RICCUCCI S., BONCIANI F. & MANCINI S. (2011) - *Stability analysis of "Grotta delle Felci" Cliff (Capri Island, Italy): structural, engineering-geological, photogrammetric surveys and laser scanning*. Bulletin of Engineering Geology and the Environment, **70** (4): 549-557.
- SALVINI R., FIRPO G., CARMIGNANI L., FANTOZZI P.L., AIELLO E., CORNIANI M., MASSA G., BONCIANI F., LAPINI M. & COCCA P. (2007a) - *Studio della frana di Guadine (MS) attraverso fotogrammetria digitale terrestre, laser scanner e rilievi geologici*. 11° Conferenza Nazionale ASITA, Turin, Italy, November 6-9, II: 1937-1942.
- SALVINI R., FIRPO G., CARMIGNANI L., FANTOZZI P.L., AIELLO E., CORNIANI M., MASSA G., BONCIANI F., LAPINI M. & COCCA P. (2007b) - *Study of the Guadine rockfall (Massa district, Italy) by digital terrestrial photogrammetry, laser scanner and geological, geomorphological and geomechanical surveys*. Geoitalia 2007, VI Forum Italiano di Scienze della Terra, Rimini, Italy, September 12-14, 2: 205.

- SALVINI R., FRANCONI M., RICCUCCI S., BONCIANI F. & CALLEGARI I. (2013) - *Photogrammetry and laser scanning for analyzing slope stability and rock fall runoff along the Domodossola-Iselle railway, the Italian Alps*. *Geomorphology*, **185**: 110-122.
- STURZENEGGER M., STEAD D., BEVERIDGE A. & LEE S. (2009) - *Long-range terrestrial digital photogrammetry for discontinuity characterization at Palabora open-pit mine*. In DIEDERICHS M. & GRASSELLI G. EDS. "ROCKENG09: Proceedings of the 3<sup>rd</sup> CANUS Rock Mechanics Symposium", Toronto, paper 3984, 10 pp.
- STURZENEGGER M. & STEAD D. (2009) - *Close-range terrestrial digital photogrammetry and terrestrial laser scanning for discontinuity characterization on rock cuts*. *Engineering Geology*, **106**: 163-182.
- TAMBURI A. (2008) - *The use of terrestrial laser scanner for the geomechanical characterization of inaccessible unstable rock slopes*. Workshop on "Landslide monitoring techniques based on remote sensing tools", EC FP6 Galahad project, Madrid, October 17, 2008.
- TOPPE R. (1987) - *Terrain models - a tool for natural hazard mapping*. Proceedings of the Davos Symposium. Avalanche formation, movement and effects. IAHS Publication, **162**: 629-638.
- WICKENS E.H. & BARTON N.R. (1971) - *The application of photogrammetry to the stability of excavated rock slopes*. *The Photogrammetric Record*, **7** (37): 46-54.